Оптический журнал

Оптическое приборостроение

DOI:10.17586/1023-5086-2018-85-10-56-60

A new matrix solution of the phase correlation technique in a brillouin dynamic grating sensor

Abdollah Malakzadeh, Mohsen Mansoursamaei

Imam Hossein University, Physics Group, Basic Sciences department, Tehran, Iran

E-mail: afard77@gmail.com

Submitted 24.10.2018

In phase correlation measurement technique of Brillouin dynamic grating sensors, two counter-propagating pump waves are modulated by a pseudo-random bit sequence (PRBS) which applies a random phase shift of either 0 or π with a specified period. In order to define the sensing length and spatial resolution, the shape of the correlation peak has to be found. So far, many methods have been used to demonstrate the phase correlation but, they often require several lengthy and sometimes complicated mathematical assumptions and equations. One of the techniques which has the best reported spatial resolution, is called the time gated phase correlation technique. We introduce a novel method based on matrix solution to show the phase modulation in the phase correlation technique. It is a straightforward and an intuitive pattern to visualize the phase modulation of the pumps and to attain the shape of the phase correlation peaks. Finally, the results of the matrix method are completely consistent with the previous results.

Keywords: *distributed fiber sensor, Brillouin dynamic grating (BDG), BDG sensor, matrix method, phase correlation technique.*

OCIS codes: *060.2370, 060.5060, 060.4370.*

Новое матричное решение в методе фазовой корреляции для датчика на основе динамических бриллюэновских решёток

Abdollah Malakzadeh, Mohsen Mansoursamaei

При проведении измерений сигналов от датчиков на основе динамических бриллюэновских решёток с использованием метода фазовой корреляции производится модуляция двух встречных волн накачки псевдослучайной последовательностью битов с наложением случайного фазового сдвига со значениями 0 или π с заданным периодом. Для определения измеряемого интервала длины и пространственного разрешения необходимо определить форму корреляционного пика. Многие из применяемых для этого способов требуют длительных расчётов и зачастую сложных математических процедур. Одним из обсуждаемых способов, обеспечивающим наилучшее пространственное разрешение, является использование временнóго стробирования. Предложен новый метод проведения вычислений с использованием матричного решения, основанный на прямом и интуитивно понятном подходе к визуализации процедуры фазовой модуляции волн накачки, позволяющий находить форму корреляционного пика. Показано соответствие полученных результатов с ранее опубликованными.

Ключевые слова: *распределенный волоконный датчик, динамическая бриллюэновская решетка, матричный метод, техника фазовой корреляции.*

INTRODUCTION

The spatial resolution and sensing length are the most important parameters in distributed fiber sensors. Among the distributed fiber sensors, Brillouin scattering based ones have usually the higher spatial resolution [1, 2]. Brillouin dynamic grating (BDG) was introduced first time in 2008 by Song et al [3] and attracted considerable attentions as a novel idea in distributed fiber optic sensors [4–6]. The BDG spectra is measured by correlation-domain measurement technique [7, 8]. In this technique, sensing length is determined by distance between two consecutive correlation peaks and spatial resolution is determined by the full width at half maximum (FWHM) of one of the peaks [9].

In the first years, several designs were proposed based on the frequency correlation technique for BDG sensor, which each improved slightly the sensor parameters, but the spatial resolution and maximum sensing length of this techniques was not remarkable [9–12]. Later the phase correlation technique was introduced in BDG sensors [13–16] which the time-gated phase-correlation technique by Denisov et al [13, 14] had the best of results and the spatial resolution of 9 mm and 14 mm over a 295 m and 460 m sensing length was achieved using phase-correlation of this method, respectively. Long mathematical relations and lengthy signals processing of the conventional method in phase correlation technique encourage us to propose a new and straightforward matrix method to overcome these problems.

2. PHASECORRELATION TECHNIQUE

In the phase correlation technique, a pseudo-random bit sequence (PRBS) applies a periodic and random phase shift of either 0 or π to modulate the pumps phases. The two counter propagating pump waves inside the fiber have similar periodic and random phases. Each period is divided into N_{bits} equal parts called a bit and occupies a specified duration (T_{bit}). In this technique, pump 1 is a pulsed laser and pump 2 is continuous wave laser. As the pumps cross through each other, the pump 1 pulse meets several phase patterns in a periodic series of the continuous wave pump 2 laser similar to its own phase pattern, resulting multiple correlation peaks inside the fiber. To find how the acoustic wave changes in time and how it interacts with the pump waves, a modulation function f_{PRBS} is defined as [14]:

$$f_{\text{PRBS}}(t)=\sum_q \xi_q \Pi\left(\left(t-qT_{\text{bit}}\right)/T_{\text{bit}}\right), \quad (1)$$

where ξ_q is a pseudo-random sequence of zeroes and ones with the period of N_{bits}, therefore $\xi_q \equiv \xi_{q+N\text{bits}}$, q is the number of bits and Π is a rectangular function between zero and one. In order to define the sensing length and spatial resolution in phase correlation technique, the shape of correlation peak has to be calculated and found. Several mathematical assumptions and equations are required to obtain the acoustic wave shape. In order to obtaining the force driving, amplitude, of the acoustic wave, it is necessary to find the time average of the square of the total electrical field ($\langle E^2\rangle$) in the strictive pressure equation. This pressure comes from the electrostriction effect due to the presence of two optical waves. The strictive pressure is the contribution to the pressure of the material which is due to the presence of the electric field. As a result, it is required to find the behavior of the phase terms of the exponent's argument of $\langle E^2\rangle$ [14]:

$$\langle E^2\rangle \approx \left\langle \exp\left\{i\pi\left[f_{\text{PRBS}}\left(t-t_{p1}(z)\right)-\right.\right.\right.$$
$$\left.\left.\left.-f_{\text{PRBS}}\left(t-t_{p2}(z)\right)\right]\right\}\right\rangle, \quad (2)$$

where t_{p1} and t_{p2} are the propagation time for the pump 1 and the pump 2. For these purposes, each bit is divided into parts with Δt time length and the average force of each part of the bits depends on the distance of the part from the correlation peak center. This means that outside of the correlation peak the forces driving the acoustic wave average out to zero. Eventually, the average value of these terms gives the average of the rectangular pulse train, which leads to a triangular shape of correlation peak. Due to the complexity of these methods, in this article we propose a straightforward and an intuitive matrix method to visualize the phase modulation of the pumps and to get the shape of the phase correlation peaks. Both methods show the correlation peak has a triangular shape although the proposed matrix method is more intuitive and tangible. It should be noted that the matrix method is a common method in many fields of fiber optic sensors [17].

3. MATRIX SOLUTION OF PHASE CORRELATION

In our new method, each pump is represented by a matrix. Pump 1 Matrix's columns equals to the number of bits, and if the fiber length is longer than the length of the modulation period, the subsequent modulations will appear in the next columns of the first row. Furthermore in order to observe the phase modulation of the pump 1 and pump 2 at different times, the rows of these matrices are defined so that each row is as many as one bit ahead of its upper row, i.e. each row is head of its previous row as much as T_{bit}. The number of rows is related to the times that the acoustic wave amplitude must be checked to be realized as a correlation peak. If the rows are not enough, we will observe that the SNR value decreases and the peaks cannot be seen. With large number of rows, the computation becomes very time consuming and sometimes impossible. The phases of both pumps are similarly modulated. Since the pumps contour-propagate in the fiber to generate the dynamic grating, the pump 2 (p_2) matrix form is mirrored of the pump 1 (p_1) shown as

$$p1=\begin{bmatrix} 0\ \pi\ \pi\ \pi \ldots\ldots\ldots.0\ldots\ldots\ldots\ 0\ 0\ 0\ \pi \\ \pi\ \pi\ \pi\ 0 \ldots\ldots\ldots.\pi\ldots\ldots\ldots 0\ 0\ \pi\ \pi \\ \pi\ \pi\ 0\ \pi \ldots\ldots\ldots.0\ldots\ldots\ldots 0\ \pi\ \pi\ 0 \\ \ldots\ldots\ldots\ldots\ldots\ldots.0\ldots\ldots\ldots\ldots\ldots\ldots. \\ \ldots\ldots\ldots\ldots\ldots\ldots.\pi\ldots\ldots\ldots\ldots\ldots\ldots \\ \ldots\ldots\ldots\ldots\ldots\ldots.\pi\ldots\ldots\ldots\ldots\ldots\ldots \\ 0\ \pi\ \pi\ \pi \ldots\ldots\ldots..0\ldots\ldots\ldots\pi\ 0\ \pi\ 0 \end{bmatrix},$$

$$p2=\begin{bmatrix} \pi\ 0\ 0\ 0 \ldots\ldots\ldots.0\ldots\ldots\ldots\ \pi\ \pi\ \pi\ 0 \\ \pi\ \pi\ 0\ 0 \ldots\ldots\ldots.\pi\ldots\ldots\ldots 0\ \pi\ \pi\ \pi \\ 0\ \pi\ \pi\ 0 \ldots\ldots\ldots.0\ldots\ldots\ldots\pi\ 0\ \pi\ \pi \\ \ldots\ldots\ldots\ldots\ldots\ldots.0\ldots\ldots\ldots\ldots\ldots\ldots \\ \ldots\ldots\ldots\ldots\ldots\ldots.\pi\ldots\ldots\ldots\ldots\ldots\ldots \\ \ldots\ldots\ldots\ldots\ldots\ldots.\pi\ldots\ldots\ldots\ldots\ldots\ldots \\ 0\ \pi\ 0\ \pi \ldots\ldots\ldots.0\ldots\ldots\ldots\pi\ \pi\ \pi\ 0 \end{bmatrix}.$$

If there is no time delay between the pumps, they will arrive in the middle of fiber simultaneously. At first moment, they face each other and after half bit of time ($T_{bit}/2$), they overlap in the middle of fiber. This moment of collision of two matrices is shown schematically in Fig. 1.

They cross each other and after next T_{bit}, their overlap can schematically be displayed in Fig. 2.

It shows that the overlap only at the center is maximum and in the other places, it is completely random. In the middle of fiber, the phase difference between the pumps is always a constant value over time. The phase difference between the pumps, when they completely overlap, can be represented as:

$$p_{12}=p_1-p_2=\pi x\begin{bmatrix} -1\ 1\ 1\ 1\ \ldots..0\ldots..\ -1\ -1\ -1\ 1 \\ 0\ 0\ 1\ 0\ \ldots..0\ldots..\ \ 0\ -1\ \ 0\ \ 0 \\ 1\ \ 0-1\ 0\ \ldots..0\ldots..\ -1\ \ 1\ \ 0-1 \\ \ldots\ldots\ldots\ldots\ldots\ldots.0\ldots\ldots\ldots\ldots\ldots\ldots\ldots \\ \ldots\ldots\ldots\ldots\ldots\ldots.0\ldots\ldots\ldots\ldots\ldots\ldots\ldots \\ \ldots\ldots\ldots\ldots\ldots\ldots.0\ldots\ldots\ldots\ldots\ldots\ldots\ldots \\ 0\ 0\ 1\ 0\ \ldots\ldots0\ldots\ldots\ 0\ \ -1\ \ 0\ \ 0 \end{bmatrix}.$$

Considering the equation (2), in order to obtain the acoustic wave amplitude in each point of the fiber, we need to insert the phase difference between the pumps in the acoustic wave equation. According to the matrix p_{12}, this difference is equal to zero or ± 1. In the correlation peak point, the phase difference between the pumps remains constant over time, i.e. in the correlation peak point, the exponential part is always zero and this equation becomes maximum [18]. Elsewhere the phase difference between the pumps is random and not necessarily zero, therefore the acoustic wave amplitude is random there leading to a noisy distribution.

$$\left[\begin{array}{ccccccc} 0\ \ \pi\ \ \pi\ \ \pi\ \ \ldots.0\ldots.\ 0\ \ 0\ \ 0 \\ \pi\ \ \pi\ \ \pi\ \ 0\ \ \ldots.\pi\ldots.\ 0\ \ 0\ \ \pi \\ \pi\ \ \pi\ \ 0\ \ \pi\ \ \ldots.0\ldots.\ 0\ \ \pi\ \ \pi \\ \ldots\ldots\ldots\ldots\ldots.0\ldots\ldots\ldots\ldots \\ \ldots\ldots\ldots\ldots\ldots.\pi\ldots\ldots\ldots\ldots \\ \ldots\ldots\ldots\ldots\ldots.\pi\ldots\ldots\ldots\ldots \\ 0\ \ \pi\ \ \pi\ \ \pi\ \ \ldots.0\ldots.\ \pi\ \ 0\ \ \pi \end{array}\left[\begin{array}{c} \pi \\ \pi \\ 0 \\ \ldots \\ \ldots \\ \ldots \\ 0 \end{array}\right]\begin{array}{c} 0\ \ 0\ \ 0\ \ldots.0\ldots.\ \pi\ \ \pi\ \ \pi\ \ 0 \\ \pi\ \ 0\ \ 0\ \ldots.\pi\ldots.\ 0\ \ \pi\ \ \pi\ \ \pi \\ \pi\ \ \pi\ \ 0\ \ldots.0\ldots.\ \pi\ \ 0\ \ \pi\ \ \pi \\ \ldots\ldots\ldots\ldots.0\ldots\ldots\ldots\ldots\ldots \\ \ldots\ldots\ldots\ldots.\pi\ldots\ldots\ldots\ldots\ldots \\ \ldots\ldots\ldots\ldots.\pi\ldots\ldots\ldots\ldots\ldots \\ \pi\ \ 0\ \ \pi\ \ldots.0\ldots.\ \pi\ \ \pi\ \ \pi\ \ 0 \end{array}\right]$$

Fig. 1. Overlap of the two matrices (pumps) after time $T_{bit}/2$.

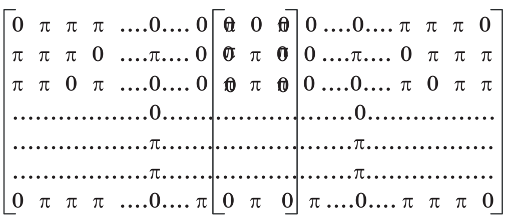

Fig. 2. Overlap of the two matrices (pumps) after time $3T_{bit}/2$.

4. RESULTS AND DISCUSSIONS

The sensing length and spatial resolution of the created BDG sensor are obtained by drawing the acoustic wave in normalized form. They can also be calculated as

$$x=\frac{cN_{bit}T_{bit}}{2n_{eff}},\ \Delta z=\frac{cT_{bit}}{2n_{eff}}. \qquad (3)$$

where n_{eff} is the effective refractive index of the fiber and c is the light velocity in vacuum. According to the optimal SNR level, using the PRBS duration (N_{bits}) and bit duration (T_{bit}) as 32767 bits (2^{15}–1) and 140 ps [14], we obtain the sensing length and spatial resolution of 460 m and 14 mm by the conventional phase correlation technique, respectively.

The results of our simulation are presented in the Fig. 3 (a) and (b). As shown, the distance between two consecutive correlation peaks (sensing length) and the FWHM of the correlation peaks (spatial resolution) obtained by the matrix method are fully consistent with the previous complicated phase correlation technique.

In another optimal case, for the bit duration of 90 ps and the previous PRBS duration [14], the sensing length of 295 m and spatial resolution of 9 mm will be achieved which is quite like consistent with our method in Fig. 4.

The results of our simulation are presented in the Fig. 4 (a) and (b). As also see in this example,

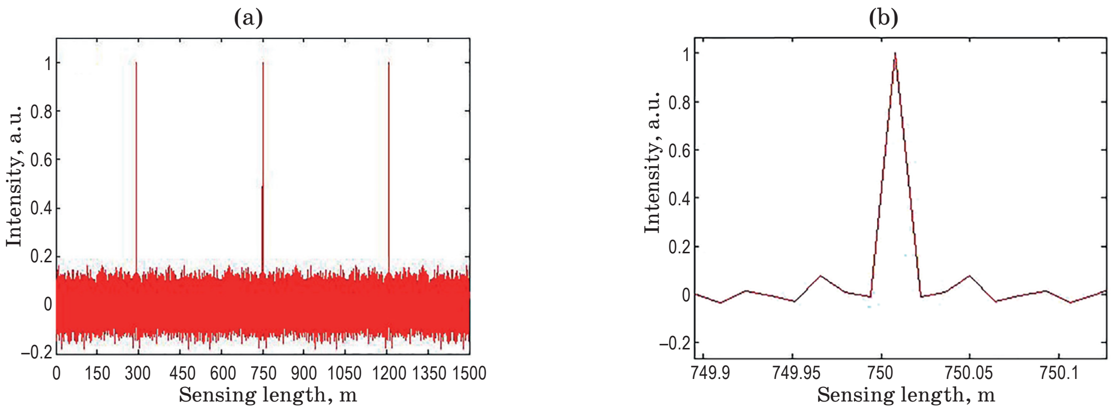

Fig. 3. Phase correlation trace for 140 ps bit duration a) whole simulation range b) a single peak to show spatial resolution.

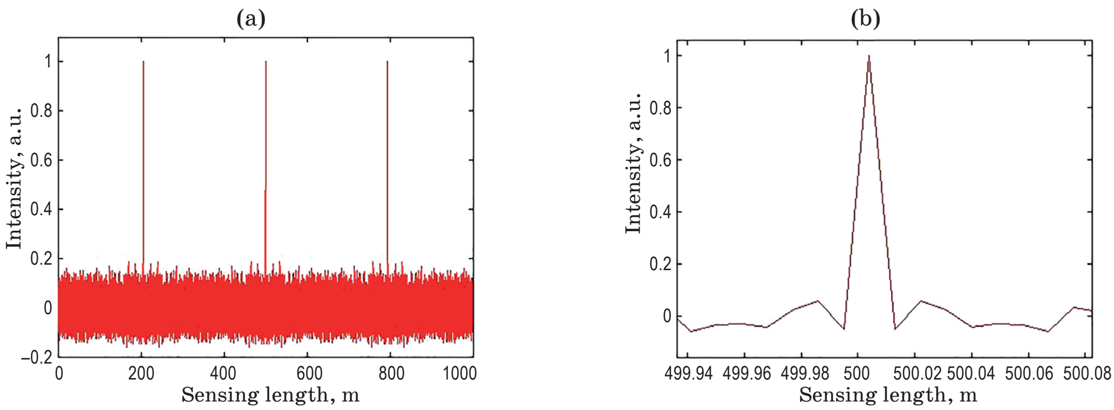

Fig. 4. Phase correlation trace for 90 ps bit duration a) whole simulation range b) a single peak to show spatial resolution.

the sensing length and the spatial resolution are obtained by the matrix method are exactly consistent with the previous complicated phase correlation technique.

5. CONCLUSION

Due to the low spatial resolution of distributed fiber sensors, the BDG sensor was innovated to enhance the spatial resolution of the sensors. Frequency and phase correlation techniques were used to improve the properties of these sensors. Spatial resolution and maximum sensing length of frequency correlation were limited and on the other hand the phase correlation consists of lengthy and tedious relations and signal processing. We propose a novel matrix solution, straightforward method to visualize the phase modulation of the pump waves. Its results are consistence with the results of conventional phase correlation.

Authors would like to thank Mrs. S.N. Jouybari for her advices and discussion about the BDG issues.

REFERENCES

1. *Bao X., Chen L.* Recent progress in distributed fiber optic sensors // Sensors. 2012. V. 12(7). P. 8601–8639.

2. *Minardo A., Coscetta A., Bernini R., Zeni L.* Heterodyne slope-assisted Brillouin optical time-domain analysis for dynamic strain measurements // Journal of Optics. 2016. V. 18(2). P. 025606.

3. *Song K.Y., Zou W., He Z., Hotate K.* All-optical dynamic grating generation based on Brillouin scattering in polarization-maintaining fiber // Opt. Lett. 2008. V. 33(9). P. 926–928.

4. *Kim Y.H., Song K.Y.* OTDR based on Brillouin dynamic grating in an e-core two-mode fiber for simultaneous measurement of strain and temperature distribution // Optical Fiber Sensors Conference (OFS) in Jeju Island, South Korea. 25 th. IEEE. 2017. V. 10323. P. 103230S-1–4.

5. *Bergman A., Langer T., Tur M.* Slope-assisted complementary-correlation optical time-domain analysis of Brillouin dynamic gratings for high sensitivity, high spatial resolution, fast and distributed fiber strain sensing // Fifth Asia-Pacific Optical Sensors Conference in Jeju Island, South Korea. International Society for Optics and Photonics. 2015. V. 9655. P. 96550.

6. *Song K.Y., Hotate K., Zou W., He Z.* Applications of Brillouin dynamic grating to distributed fiber sensors // Journal of Lightwave Technology. 2017. V. 35(16). P. 3268–3280.

7. *Choi B.H., Kwon I.B.* Brillouin optical correlation analysis system using a simplified frequency-modulated time division method // Optical Engineering. 2014. V. 53(1). P. 016105.

8. *Lee H., Mizuno Y., Nakamura K.* Measurement sensitivity dependencies on incident power and spatial resolution in slope-assisted Brillouin optical correlation-domain reflectometry // Sensors and Actuators A: Physical. 2017. V. 268. P. 68–71.

9. *Chin S., Primerov N., Thévenaz L.* Sub-centimeter spatial resolution in distributed fiber sensing based on dynamic Brillouin grating in optical fibers // IEEE Sensors. 2012. V. 12(1). P. 189–194.

10. *Teng L., Dong Y., Zhou D., Bao X., Chen L.* Distributed hydrostatic pressure sensor using a thin-diameter and polarization-maintaining photonics crystal fiber based on Brillouin dynamic gratings // Optical Fiber Sensors Conference (OFS) in Jeju Island, South Korea. 25 th. IEEE. 2017. V. 10323. P. 103236Q-1–4.

11. *Jouybari S.N., Latifi H., Farahi F.* Reflection spectrum analysis of stimulated Brillouin scattering dynamic grating // Measurement Science and Technology. 2012. V. 23(8). P. 085203.

12. *Song K.Y., Chin S., Primerov N., Thévenaz L.* Time-domain distributed fiber sensor with 1 cm spatial resolution based on Brillouin dynamic grating // Journal of Lightwave Technology. 2010. V. 28(14). P. 2062–2067.

13. *Denisov A., Soto M.A., Thévenaz L.* Going beyond 1000000 resolved points in a Brillouin distributed fiber sensor: theoretical analysis and experimental demonstration // Light: Science & Applications. 2016. V. 5(5). P. e16074.

14. *Denisov A.* Brillouin dynamic gratings in optical fibers for distributed sensing and advanced optical signal processing // Ph.D. Thesis. École Polytechnique Federale de Lausanne, 2015. P. 17–22.

15. *Bergman A., Langer T., abd Tur M.* Phase-based, high spatial resolution and distributed, static and dynamic strain sensing using Brillouin dynamic gratings in optical fibers // Optics express. 2017. V. 25(5). P. 5376–5388.

16. *Denisov A., Soto M.A., Thévenaz L.* 1’000’000 resolved points along a Brillouin distributed fibre sensor // Proc. SPIE. 2014. V. 9157. No. EPFL-CONF-199500. P. 9157D2.

17. *Khalid K.S., Zafrullah M., Bilal S.M., Mirza M.A.* Simulation and analysis of Gaussian apodized fiber Bragg grating strain sensor // Journal of Optical Technology. 2012. V. 79(10). P. 667–673.

18. *Jouybari S.N., Latifi H., Ahmadlou A., Karami M.* Spatial resolution enhancement for Brillouin optical time domain analysis distributed sensor by use of correlation peak // SPIE Europe Optical Metrology. International Society for Optics and Photonics. 2009. V. 7389. P. 73892T-1–7.